Submitted to ACTA MECHANICA

Transient response of coplanar interfacial cracks between two dissimilar piezoelectric strips under anti-plane mechanical and in-plane electrical impacts

R. K. L. Su*, W. J. Feng, J. X. Liu, Z.Z. Zou

Summary The linear piezoelectricity theory is applied to investigate the dynamic response of two coplanar interface cracks between two dissimilar piezoelectric strips subjected to the mechanical and electrical impacts. Two kinds of electric boundary conditions on crack surfaces, i.e. electric impermeable and electric permeable, are adopted. Laplace and Fourier transforms and dislocation density functions are employed to reduce the mixed boundary value problem to Cauchy singular integral equations in Laplace transform domain, which are solved numerically. Numerical results show the effects of electrical load, geometry criterion of piezoelectric strips, relative crack position and material property parameter on dynamic stress intensity factor and/or energy release rate.

Keywords coplanar interface cracks, dissimilar piezoelectric strips, singular integral equations, dynamic stress intensity factor, dynamic energy release rate

1 Introduction

* Corresponding author: Fax: (852) 2559 5337; Tel: (852) 2859 2648; E-mail: klsu@hkucc.hku.hk

Due to the intrinsic coupling characteristics between electric and elastic behaviors, piezoelectric materials have been used widely in technology such as transducers, actuators, sensors, etc. Studies on electroelastic problems of a piezoelectric material with cracks in the framework of the theory of piezoelectricity were initiated by Parton [1] and Deeg [2]. Since their pioneering works, the problem of the determination of electroelastic field under different boundary conditions was investigated by a number of researchers and has become the topic of intensive research in recent years.

The dynamic response problem of mechanical and electrical behaviors in a piezoelectric material under various time-dependent loads is of great importance in some practical applications such as in the detection of ultrasonic waves and has recently received much attention. Great progress in this area has been made, for example, fundamental solutions and general solutions of dynamic piezoelectricity equations for piezoelectric materials were solved in Khutoryansky and Sosa [3] and Ding et al. [4], respectively. The dynamic fracture of piezoelectric materials has been investigated in the quasielectrostatic approximation by Dascalu and Maugin [5], who obtained asymptotic expressions for crack-tip field by using a complex-variable approach and, in particular, determined the crack-tip trajectory by numerically solving a resulting differential equation for a mode-III crack of finite length extending symmetrically along the crack line. Li and Mataga [6], [7] studied a pair of concentrated longitudinal shear loads that suddenly act on the crack surfaces and move at constant velocity along the crack surface far away from the crack tip, and derived the dependence of the field intensity factors and the energy release rate on the

moving velocity for an electrode crack and a vacuum crack, respectively. For a piezoelectric medium or a piezoelectric strip containing an impermeable finite crack or two coplanar cracks subjected to impact loads, numerical stress intensity factors have been determined by the numerical solution of a Fredholm integral equation [8]-[11]. Wang and Yu [12] studied the mode-III problem of a crack in piezoelectric strip subjected to the mechanical and electrical impacts by solving numerically resulting Cauchy integral equations. Wang et al. [13] investigated the multiple impermeable crack problem for multilayered piezoelectric materials, and gave some numerical results under purely mechanical or electrical load, and Kwon and Lee [14] analyzed the transient response of a rectangular piezoelectric body with a center crack. Recently, Li [15] and Li and Fan [16] investigated the transient response of a piezoelectric material with a semi-infinite impermeable mode-III crack under impact loads and the problem of a through permeable crack situated in the mid-plane of a piezoelectric strip under anti-plane impact loads, respectively. For scattering of incident waves from the crack, Shindo et al. [17], and Narita and Shindo [18] investigated, respectively, the scattering of Love waves by an edge crack in piezoelectric layered media, and the dynamic response of a cracked dielectric medium in a uniform electric field. Wang and Yu [19] analyzed the scattering of SH waves by an arc-shaped crack between a cylindrical piezoelectric inclusion and matrix, and obtained the corresponding scattered far field pattern and scattered cross section.

In this paper, we study the transient response of two coplanar interface cracks between two dissimilar piezoelectric strips subjected to anti-plane mechanical and

electrical impacts under two different crack surface conditions. In the first case, the cracks are impermeable for electric fields with the surface condition as [20]

$$D_n^+ = D_n^- = 0, \tag{1}$$

and in the second case, the cracks are permeable for electric fields with the surface condition as [1]

$$D_n^+ = D_n^-, \ \phi^+ = \phi^-, \tag{2}$$

where D_n is the electric displacement in the direction normal to the crack surface, and ϕ denotes the electric potential. Integral transforms and dislocation density functions are used to reduce the problem to singular integral equations that can be solved numerically.

2. Basic equations

Consider two mode-III Griffith cracks of the same length along the interface between two bonded transversely isotropic piezoelectric strips occupying $0 < y < h_1$ and $-h_2 < y < 0$, respectively, with their basal planes perpendicular to the z axis, as shown in Fig. 1. The cracks are located along the x axis from $-b$ to $-a$ and from a to b. The antiplane shear impact and the electric displacement impact are imposed on the crack surfaces at $t = 0$. In this case, only the out-of-plane elastic displacements and the in-plane electric field are non-zero, that is

$$u_{x(j)} = u_{y(j)} = 0, \quad u_{z(j)} = w_{(j)}(x, y, t), \quad j = 1,2, \tag{3}$$

$$E_{x(j)} = E_{x(j)}(x, y, t), \quad E_{y(j)} = E_{y(j)}(x, y, t), \quad E_{z(j)} = 0, \quad j = 1,2, \tag{4}$$

where the quantities with the subscript (j), $j=1,2$ denote the corresponding quantities in the upper and lower strips, respectively. (u_x, u_y, u_z) and (E_x, E_y, E_z) are the components of the displacement and the electric field vectors, respectively, and $E_i\ (i=x,y,z)$ are related to the electric potential ϕ as $E_i = -\phi_{,i}$. The constitutive relations are as follows:

$$\sigma_{zy(j)} = c_{44(j)}\,\partial w_{(j)}/\partial y + e_{15(j)}\,\partial \phi_{(j)}/\partial y\ , \quad j=1,2, \tag{5}$$

$$D_{y(j)} = e_{15(j)}\,\partial w_{(j)}/\partial y - \varepsilon_{11(j)}\,\partial \phi_{(j)}/\partial y\ , \quad j=1,2, \tag{6}$$

where $\phi_{(1)}$ and $\phi_{(2)}$ denote the electric potentials in the upper and lower strips, respectively, $\sigma_{zy(j)}$ and $D_{y(j)}$ are the corresponding stress and electric displacements, respectively, and $c_{44(j)}$, $\varepsilon_{11(j)}$, $e_{15(j)}$ are the elastic, the dielectric and the piezoelectric constants, respectively. The governing equations of dynamic antiplane piezoelectricity are

$$c_{44(j)}\nabla^2 w_{(j)} + e_{15(j)}\nabla^2 \phi_{(j)} = \rho_{(j)}\frac{\partial^2 w_{(j)}}{\partial t^2}\ , \quad j=1,2, \tag{7}$$

$$e_{15(j)}\nabla^2 w_{(j)} - \varepsilon_{11(j)}\nabla^2 \phi_{(j)} = 0\,, \quad j=1,2, \tag{8}$$

where ∇^2 is the two-dimensional Laplace operator, i.e. $\nabla^2 = \partial^2/\partial x^2 + \partial^2/\partial y^2$.

The boundary conditions for the impermeable case are

$$\sigma_{zy(1)}(x,0,t) = \sigma_{zy(2)}(x,0,t) = -\tau_0 H(t), \quad a<|x|<b\,, \tag{9}$$

$$D_{y(1)}(x,0,t) = D_{y(2)}(x,0,t) = -D_0 H(t), \quad a<|x|<b\,, \tag{10}$$

$$w_{(1)}(x,0,t) = w_{(2)}(x,0,t)\,, \qquad o\le|x|\le a\,, \quad |x|\ge b\,, \tag{11}$$

$$\phi_{(1)}(x,0,t) = \phi_{(2)}(x,0,t)\,, \qquad o\le|x|\le a\,, \quad |x|\ge b\,, \tag{12}$$

$$\sigma_{zy(1)}(x,0,t) = \sigma_{zy(2)}(x,0,t)\,, \quad -\infty<x<+\infty\,, \tag{13}$$

$$D_{y(1)}(x,0,t) = D_{y(2)}(x,0,t)\,, \quad -\infty<x<+\infty\,, \tag{14}$$

$$\sigma_{zy(1)}(x,h_1,t)=0,\qquad -\infty<x<+\infty, \tag{15}$$

$$\sigma_{zy(2)}(x,-h_2,t)=0,\quad -\infty<x<+\infty, \tag{16}$$

$$D_{y(1)}(x,h_1,t)=0,\qquad -\infty<x<+\infty, \tag{17}$$

$$D_{y(2)}(x,-h_2,t)=0,\quad -\infty<x<+\infty, \tag{18}$$

where $H(t)$ denotes the Heaviside unit step function. For the electric permeable case , the boundary conditions become

$$\sigma_{zy(1)}(x,0,t)=\sigma_{zy(2)}(x,0,t)=-\tau_0 H(t),\quad a<|x|<b, \tag{19}$$

$$w_{(1)}(x,0,t)=w_{(2)}(x,0,t),\qquad o\le|x|\le a,\quad |x|\ge b, \tag{20}$$

$$\sigma_{zy(1)}(x,0,t)=\sigma_{zy(2)}(x,0,t),\quad -\infty<x<+\infty, \tag{21}$$

$$\phi_{(1)}(x,0,t)=\phi_{(2)}(x,0,t),\qquad -\infty<x<+\infty, \tag{22}$$

$$D_{y(1)}(x,0,t)=D_{y(2)}(x,0,t),\quad -\infty<x<+\infty, \tag{23}$$

$$\sigma_{zy(1)}(x,h_1,t)=0,\qquad -\infty<x<+\infty, \tag{24}$$

$$\sigma_{zy(2)}(x,-h_2,t)=0,\quad -\infty<x<+\infty, \tag{25}$$

$$D_{y(1)}(x,h_1,t)=0,\qquad -\infty<x<+\infty, \tag{26}$$

$$D_{y(2)}(x,-h_2,t)=0,\quad -\infty<x<+\infty, \tag{27}$$

and the electric displacements on the crack surfaces $D_{y(j)}(x,0,t)$ consist of two parts, the imposed $-D_0H(t)$ and the unknown caused by $-\tau_0H(t)$.

Introduce Laplace transform as follows:

$$w_{(j)}{}^{*}(x,y,p)=\int_0^{+\infty}w_{(j)}(x,y,t)\exp(-pt)dt, \tag{28}$$

$$\phi_{(j)}{}^{*}(x,y,p)=\int_0^{+\infty}\phi_{(j)}(x,y,t)\exp(-pt)dt, \tag{29}$$

$$w_{(j)}(x,y,t)=\frac{1}{2\pi i}\int_{Br}w_{(j)}{}^{*}(x,y,p)\exp(pt)dp, \tag{30}$$

$$\phi_{(j)}(x,y,t)=\frac{1}{2\pi i}\int_{Br}\phi_{(j)}{}^{*}(x,y,p)\exp(pt)dp, \tag{31}$$

in which Br denotes the Bromwich path of integration. Noting that both $w_{(j)}$ and $\phi_{(j)}$ are even functions with respect to variable x, the Fourier cosine transforms are applied to give the solutions as

$$w_{(j)}^{*}(x,y,p)=\frac{2}{\pi}\int_0^{+\infty}\left[A_{(j)}(s,p)\exp\left(-\alpha_{(j)}y\right)+B_{(j)}(s,p)\exp\left(\alpha_{(j)}y\right)\right]\cos(sx)ds,\ j=1,2, \tag{32}$$

$$\begin{aligned}\phi_{(j)}^{*}(x,y,p)=&\frac{e_{15(j)}}{\varepsilon_{11(j)}}w_{(j)}^{*}(x,y,p)\\&+\frac{2}{\pi}\int_0^{+\infty}\left[C_{(j)}(s,p)\exp(-sy)+D_{(j)}(s,p)\exp(sy)\right]\cos(sx)ds,\end{aligned}\qquad j=1,2, \tag{33}$$

where $A_{(j)}$, $B_{(j)}$, $C_{(j)}$ and $D_{(j)}$ are the unknowns to be solved and

$$\alpha_{(j)}=\sqrt{s^2+\frac{p^2}{c_{T(j)}^{\ 2}}},\quad c_{T(j)}=\sqrt{\frac{\tilde{c}_{44(j)}}{\rho_{(j)}}},\quad \tilde{c}_{44(j)}=c_{44(j)}+e_{15(j)}^{\ 2}/\varepsilon_{11(j)}. \tag{34}$$

We proceed with the impermeable case. In Laplace transform domain, defining dislocation functions as

$$\Delta w^{*}(x,p)=\begin{cases}w_{(1)}^{*}(x,0,p)-w_{(2)}^{*}(x,0,p), & a<|x|<b,\\ 0, & 0\le|x|\le a,\quad b\le|x|<\infty,\end{cases} \tag{35}$$

$$\Delta\phi^{*}(x,p)=\begin{cases}\phi_{(1)}^{*}(x,0,p)-\phi_{(2)}^{*}(x,0,p), & a<|x|<b,\\ 0, & 0\le|x|\le a,\quad b\le|x|<\infty,\end{cases} \tag{36}$$

we obtain from Eqs. (11) and (12)

$$w_{(1)}^{*}(x,0,p)-w_{(2)}^{*}(x,0,p)=\Delta w^{*}(x,p),\qquad -\infty<x<+\infty, \tag{37}$$

$$\phi_{(1)}^{*}(x,0,p)-\phi_{(2)}^{*}(x,0,p)=\Delta\phi^{*}(x,p),\qquad -\infty<x<+\infty, \tag{38}$$

Substituting Eqs. (32) and (33) into Eqs. (5) and (6) and using Eqs. (13)-(18), (37) and (38), we have

$$\begin{bmatrix} a_{11} & a_{12} & a_{13} & a_{14} & a_{15} & a_{16} & a_{17} & a_{18} \\ a_{21} & a_{22} & a_{23} & a_{24} & a_{25} & a_{26} & a_{27} & a_{28} \\ a_{31} & a_{32} & a_{33} & a_{34} & a_{35} & a_{36} & a_{37} & a_{38} \\ a_{41} & a_{42} & a_{43} & a_{44} & a_{45} & a_{46} & a_{47} & a_{48} \\ a_{51} & a_{52} & a_{53} & a_{54} & a_{55} & a_{56} & a_{57} & a_{58} \\ a_{61} & a_{62} & a_{63} & a_{64} & a_{65} & a_{66} & a_{67} & a_{68} \\ a_{71} & a_{72} & a_{73} & a_{74} & a_{75} & a_{76} & a_{77} & a_{78} \\ a_{81} & a_{82} & a_{83} & a_{84} & a_{85} & a_{86} & a_{87} & a_{88} \end{bmatrix} \begin{Bmatrix} A_{(1)} \\ B_{(1)} \\ C_{(1)} \\ D_{(1)} \\ A_{(2)} \\ B_{(2)} \\ C_{(2)} \\ D_{(2)} \end{Bmatrix} = \begin{Bmatrix} 0 \\ 0 \\ 0 \\ 0 \\ 0 \\ 0 \\ \overline{\Delta w^*}(s,p) \\ \overline{\Delta \phi^*}(s,p) \end{Bmatrix}, \tag{39}$$

where a_{ij}, which are given in Appendix A, are knowns related to s and p, and $\overline{\Delta w^*}$ and $\overline{\Delta \phi^*}$ are Fourier cosine transforms of Δw^* and $\Delta \phi^*$, respectively. According to the Cramer's rule, we get

$$A_{(1)}(s,p) = \frac{\Delta_{71}(s,p)\overline{\Delta w^*}(s,p) + \Delta_{81}(s,p)\overline{\Delta \phi^*}(s,p)}{\Delta(s,p)}, \tag{40}$$

$$B_{(1)}(s,p) = \frac{\Delta_{72}(s,p)\overline{\Delta w^*}(s,p) + \Delta_{82}(s,p)\overline{\Delta \phi^*}(s,p)}{\Delta(s,p)}, \tag{41}$$

$$C_{(1)}(s,p) = \frac{\Delta_{73}(s,p)\overline{\Delta w^*}(s,p) + \Delta_{83}(s,p)\overline{\Delta \phi^*}(s,p)}{\Delta(s,p)}, \tag{42}$$

$$D_{(1)}(s,p) = \frac{\Delta_{74}(s,p)\overline{\Delta w^*}(s,p) + \Delta_{84}(s,p)\overline{\Delta \phi^*}(s,p)}{\Delta(s,p)}, \tag{43}$$

where $\Delta(s,p)$ is the determinant of the coefficient matrix of equation system (39), and $\Delta_{71}(s,p)$, $\Delta_{72}(s,p)$, $\Delta_{73}(s,p)$, $\Delta_{74}(s,p)$, $\Delta_{81}(s,p)$, $\Delta_{82}(s,p)$, $\Delta_{83}(s,p)$ and $\Delta_{84}(s,p)$ are respectively the corresponding algebra cofactors when applying the Cramer's rule.

3. Singular integral equations and solutions

Substituting Eqs. (32) and (33) into Eqs. (5) and (6) in Laplace transform domain and using Eqs. (9), (10), (40) to (43), we have

$$\sigma_{zy}^{*}(x,0,p)=\frac{2}{\pi}\int_0^{+\infty}\frac{P_{11}(s,p)\overline{\Delta w^{*}}(s,p)+P_{12}(s,p)\overline{\Delta\phi^{*}}(s,p)}{\Delta(s,p)}\cos(sx)ds=-\frac{\tau_0}{p}, \tag{44}$$

$$D_{y}^{*}(x,0,p)=\frac{2}{\pi}\int_0^{+\infty}\frac{P_{21}(s,p)\overline{\Delta w^{*}}(s,p)+P_{22}(s,p)\overline{\Delta\phi^{*}}(s,p)}{\Delta(s,p)}\cos(sx)ds=-\frac{D_0}{p}, \tag{45}$$

where

$$P_{i1}=\frac{a_{i1}\Delta_{71}+a_{i2}\Delta_{72}+a_{i3}\Delta_{73}+a_{i4}\Delta_{74}}{\Delta(s,p)},\quad (i=1,2), \tag{46}$$

$$P_{i2}=\frac{a_{i1}\Delta_{81}+a_{i2}\Delta_{82}+a_{i3}\Delta_{83}+a_{i4}\Delta_{84}}{\Delta(s,p)},\quad (i=1,2). \tag{47}$$

Substituting $\overline{\Delta w^{*}}(s,p)$, $\overline{\Delta\phi^{*}}(s,p)$ for $\Delta w^{*}(v,p)$, $\Delta\phi^{*}(v,p)$, and using Eqs. (35) and (36), we can obtain the following singular integral equations in Laplace transform domain by by-part integration.

$$\begin{aligned}&\frac{1}{\pi}\int_a^b\frac{\gamma_{11}}{v-x}f(v,p)dv+\frac{1}{\pi}\int_a^b\frac{\gamma_{12}}{v-x}g(v,p)dv\\&+\frac{1}{\pi}\int_a^b\left[Q_{11}(v,x,p)f(v,p)+Q_{12}(v,x,p)g(v,p)\right]dv=-\frac{\tau_0}{p},\qquad a<x<b,\end{aligned} \tag{48}$$

$$\begin{aligned}&\frac{1}{\pi}\int_a^b\frac{\gamma_{21}}{v-x}f(v,p)dv+\frac{1}{\pi}\int_a^b\frac{\gamma_{22}}{v-x}g(v,p)dv\\&+\frac{1}{\pi}\int_a^b\left[Q_{21}(v,x,p)f(v,p)+Q_{22}(v,x,p)g(v,p)\right]dv=-\frac{D_0}{p},\qquad a<x<b,\end{aligned} \tag{49}$$

where $f(v,p)=\dfrac{d\Delta w^{*}(v,p)}{dv}$ and $g(v,p)=\dfrac{d\Delta\phi^{*}(v,p)}{dv}$ are called dislocation density functions, and γ_{ij} and $Q_{ij}(v,x,p)$ are, for conciseness, all given in Appendix B.

Introducing two nondimensional variables η and ς

$$v=\frac{b-a}{2}\eta+\frac{b+a}{2},\qquad x=\frac{b-a}{2}\varsigma+\frac{b+a}{2}, \tag{50}$$

Eqs. (48) and (49) become

$$\frac{1}{\pi}\int_{-1}^{1}\frac{\gamma_{11}}{\eta-\varsigma}F(\eta,p)d\eta+\frac{1}{\pi}\int_{-1}^{1}\frac{\gamma_{12}}{\eta-\varsigma}G(\eta,p)d\eta$$
$$+\frac{1}{\pi}\int_{-1}^{1}\left[\tilde{Q}_{11}(\eta,\varsigma,p)F(\eta,p)+\tilde{Q}_{12}(\eta,\varsigma,p)G(\eta,p)\right]d\eta=-\frac{\tau_0}{p},\qquad|\varsigma|<1, \tag{51}$$

$$\frac{1}{\pi}\int_{-1}^{1}\frac{\gamma_{21}}{\eta-\varsigma}F(\eta,p)d\eta+\frac{1}{\pi}\int_{-1}^{1}\frac{\gamma_{22}}{\eta-\varsigma}G(\eta,p)d\eta$$
$$+\frac{1}{\pi}\int_{-1}^{1}\left[\tilde{Q}_{21}(\eta,\varsigma,p)F(\eta,p)+\tilde{Q}_{22}(\eta,\varsigma,p)G(\eta,p)\right]d\eta=-\frac{D_0}{p},\qquad|\varsigma|<1, \tag{52}$$

where $F(\eta,p),G(\eta,p)$ and $\tilde{Q}_{ij}(\eta,\varsigma,p)$ are also given in Appendix B.

Recalling that $F(\eta,p)$ and $G(\eta,p)$ represent the derivatives of the displacement and electric potential differences with respect to v, the single-valued conditions of Eqs. (51) and (52) may be expressed as [21]

$$\int_{-1}^{1}F(\eta,p)d\eta=0, \tag{53}$$

$$\int_{-1}^{1}G(\eta,p)d\eta=0. \tag{54}$$

So far, the Cauchy singular integral Eqs. (51) and (52) and the single-valued conditions (53) and (54) have been derived. The general theory of singular integral equations shows that $F(\eta,p)$ and $G(\eta,p)$ have $-1/2$ singularity at ±1 [22]. Letting

$$F(\eta,p)=\frac{R(\eta,p)}{\sqrt{1-\eta^2}}, \tag{55}$$

$$G(\eta,p)=\frac{V(\eta,p)}{\sqrt{1-\eta^2}}, \tag{56}$$

and expanding $R(\eta,p)$, $V(\eta,p)$ in forms of Chebyshev polynomials

$$R(\eta,p)=\sum_{i=0}^{\infty}C_i(p)T_i(\eta), \tag{57}$$

$$V(\eta,p)=\sum_{i=0}^{\infty}D_i(p)T_i(\eta), \tag{58}$$

a system of linear algebraic equations can be obtained by using Gauss-Chebyshev formula [23]:

$$\sum_{j=1}^{N}\left(\frac{\gamma_{11}}{\eta_j-\varsigma_i}+\tilde{Q}_{11}(\eta_j,\varsigma_i)\right)\frac{R(\eta_j,p)}{N}+\sum_{j=1}^{N}\left(\frac{\gamma_{12}}{\eta_j-\varsigma_i}+\tilde{Q}_{12}(\eta_j,\varsigma_i)\right)\frac{V(\eta_j,p)}{N}=-\frac{\tau_0}{p}, \quad (59)$$

$$\sum_{j=1}^{N}\left(\frac{\gamma_{21}}{\eta_j-\varsigma_i}+\tilde{Q}_{21}(\eta_j,\varsigma_i)\right)\frac{R(\eta_j,p)}{N}+\sum_{j=1}^{N}\left(\frac{\gamma_{22}}{\eta_j-\varsigma_i}+\tilde{Q}_{22}(\eta_j,\varsigma_i)\right)\frac{V(\eta_j,p)}{N}=-\frac{D_0}{p}, \quad (60)$$

$$\sum_{j=1}^{N}\frac{R(\eta_j,p)}{N}=0, \quad (61)$$

$$\sum_{j=1}^{N}\frac{V(\eta_j,p)}{N}=0, \quad (62)$$

in which

$$\eta_j=\cos[(2j-1)\pi/2N], \quad j=1,2,\cdots,N, \quad (63)$$

$$\varsigma_i=\cos(i\pi/N), \quad i=1,2,\cdots,N-1, \quad (64)$$

and N is the number of the discrete points of $R(\eta,p)$ and $V(\eta,p)$ between -1 and $+1$.

The dynamic stress intensity factor (DSIF) and the dynamic electric displacement intensity factor (DEDIF) in Laplace transform domain are defined as

$$K_{\mathrm{III}b}^{*}(p)=\lim_{x\to b^{+}}\sqrt{2\pi(x-b)}\,\sigma_{zy}^{*}(x,0,p), \quad (65)$$

$$K_{Db}^{*}(b,s)=\lim_{x\to b^{+}}\sqrt{2\pi(x-b)}\,D_{y}^{*}(x,0,p), \quad (66)$$

$$K_{\mathrm{III}a}^{*}(p)=-\lim_{x\to a^{-}}\sqrt{2\pi(a-x)}\,\sigma_{zy}^{*}(x,0,p), \quad (67)$$

$$K_{Da}^{*}(b,s)=-\lim_{x\to a^{-}}\sqrt{2\pi(a-x)}\,D_{y}^{*}(x,0,p), \quad (68)$$

By the property of Chebyshev polynomials [23]

$$\frac{1}{\pi}\int_{-1}^{1}\frac{(1-\eta^2)^{-1/2}T_j(\eta)}{\eta-\varsigma}d\eta=\frac{\left[(\varsigma^2-1)^{1/2}-\varsigma\right]^j}{(-1)^{j+1}(\varsigma^2-1)^{1/2}}, \qquad |\varsigma|>1, \quad (69)$$

we obtain

$$K_{\mathrm{III}b}{}^{*}(p)=-\sqrt{\frac{b-a}{2}\pi}\left[\gamma_{11}R(1,p)+\gamma_{12}V(1,p)\right], \tag{70}$$

$$K_{Db}{}^{*}(p)=-\sqrt{\frac{b-a}{2}\pi}\left[\gamma_{21}R(1,p)+\gamma_{22}V(1,p)\right], \tag{71}$$

$$K_{\mathrm{III}a}{}^{*}(p)=\sqrt{\frac{b-a}{2}\pi}\left[\gamma_{11}R(-1,p)+\gamma_{12}V(-1,p)\right], \tag{72}$$

$$K_{Da}{}^{*}(p)=\sqrt{\frac{b-a}{2}\pi}\left[\gamma_{21}R(-1,p)+\gamma_{22}V(-1,p)\right]. \tag{73}$$

The Laplace inverse transformations of Eqs. (70) to (73) are carried out by the numerical method developed by Miller and Guy [24]. In this paper, numerical results were given within a range of $0\le c_{T(1)}t/\left((b-a)/2\right)\le 40$.

For the impermeable case, as the electrical impact is loaded, the dynamic stress intensity factor will not play the same role as in the purely elastic case. Therefore, we introduce the dynamic energy release rate (DERR) G as Pak [20] did. According to Eqs. (65), (66), (70) and (71), as $x\to b^{+}$, $\sigma_{zy}(x,0,t)$, $D_y(x,0,t)$ and $\Delta w(x,0,t)$, $\Delta\phi(x,0,t)$ can be respectively approximated as

$$\begin{Bmatrix}\sigma_{zy}(x,0,t)\\ D_y(x,0,t)\end{Bmatrix}=\frac{1}{\sqrt{2\pi(x-b)}}\begin{Bmatrix}K_{\mathrm{III}b}(t)\\ K_{Db}(t)\end{Bmatrix},\quad j=1,2, \tag{74}$$

$$\begin{Bmatrix}\Delta w(x,0,t)\\ \Delta\phi(x,0,t)\end{Bmatrix}=\sqrt{\frac{2(b-x)}{\pi}}\frac{1}{\gamma_{11}\gamma_{22}-\gamma_{12}\gamma_{21}}\begin{bmatrix}\gamma_{22} & -\gamma_{12}\\ -\gamma_{21} & \gamma_{11}\end{bmatrix}\begin{Bmatrix}K_{\mathrm{III}b}(t)\\ K_{Db}(t)\end{Bmatrix},\quad j=1,2. \tag{75}$$

Substituting Eqs. (74) and (75) into the equation of

$$G_b d_b=\int_b^{b+d_b}\frac{1}{2}\left[\sigma_{zy}(x,0,t),\,D_y(x,0,t)\right]\left[\Delta w(x-d_b,0,t),\,\Delta\phi(x-d_b,0,t)\right]^{\mathrm{T}}dx \tag{76}$$

yields

$$G_b=\frac{1}{4(\gamma_{11}\gamma_{22}-\gamma_{12}\gamma_{21})}\left[\gamma_{22}K_{\mathrm{III}b}{}^{2}(t)-(\gamma_{12}+\gamma_{21})K_{\mathrm{III}b}(t)K_{Db}(t)+\gamma_{11}K_{Db}{}^{2}(t)\right]. \tag{77}$$

Similarly, the dynamic energy release rate as $x\to a^{-}$ can also be obtained as follows

$$G_a = \frac{1}{4(\gamma_{11}\gamma_{22} - \gamma_{12}\gamma_{21})}\left[\gamma_{22}{K_{\mathrm{III}a}}^2(t) - (\gamma_{12} + \gamma_{21})K_{\mathrm{III}a}(t)K_{Da}(t) + \gamma_{11}{K_{Da}}^2(t)\right]. \quad (78)$$

For electric permeable case, the singular integral equation and the single-valued condition can be derived by a similar method as

$$\frac{1}{\pi}\int_a^b \frac{\gamma_{11}}{v-x} f(v,p)dv + \frac{1}{\pi}\int_a^b Q_{11}(v,x,p) f(v,p)dv = -\frac{\tau_0}{p}. \quad a < x < b. \quad (79)$$

$$\int_a^b f(v,p)dv = 0, \quad (80)$$

and by means of the solution of Eqs. (79) and (80), the electric displacement $D_y^*(x,0,p)$ on crack surfaces can be obtained as

$$D_y^*(x,0,p) = \frac{1}{\pi}\int_a^b \frac{\gamma_{21}}{v-x} f(v,p)dv + \frac{1}{\pi}\int_a^b Q_{21}(v,x,p) f(v,p)dv - \frac{D_0}{p}, \quad a < x < b. \quad (81)$$

The DSIF in Laplace domain and the DERR are

$$K_{\mathrm{III}b}^*(p) = -\sqrt{\pi(b-a)/2}\gamma_{11}R(1,p), \quad (82)$$

$$K_{\mathrm{III}a}^*(p) = \sqrt{\pi(b-a)/2}\gamma_{11}R(-1,p), \quad (83)$$

$$G_b = \frac{{K_{\mathrm{III}b}}^2(t)}{4\gamma_{11}}, \quad (84)$$

$$G_a = \frac{{K_{\mathrm{III}a}}^2(t)}{4\gamma_{11}}. \quad (85)$$

The analysis of the electrical permeable case shows that the imposed electric displacement impact doesn't contribute to the DSIF and the DERR. Therefore, the DERR and the DSIF are equivalent to the fracture parameters of electric permeable boundary case. In the absence of the mechanical impact, in other words, the material is in effect seamless as far as the electric field is concerned and the field will not be perturbed by the presence of the interface cracks [25].

4. Results and discussion

In this section, the DSIF and/or the DERR for various electromechanical impact loads and different geometry and property parameters with normalized time $c_{T(1)}t/c$, where $c=\dfrac{b-a}{2}$, are respectively calculated. The numerical results of DSIF is normalized by $\tau_0(\pi c)^{1/2}$ and DERR is normalized by G_0, where G_0 is defined as [20]

$$G_0=\pi c\varepsilon_{11(1)}\tau_0^{\,2}\big/\left(2c_{44(1)}\varepsilon_{11(1)}+2e_{15(1)}^{\,2}\right), \tag{86}$$

which denotes the energy release rate for the unbounded piezoelectric material subjected to static shear $-\tau_0$. The loading combination parameter λ is determined as

$$\lambda=D_0e_{15(1)}\big/\left(\tau_0\varepsilon_{11(1)}\right), \tag{87}$$

which is used to reflect the relation between the shear impact $-\tau_0H(t)$ and the electrical impact $-D_0H(t)$. The upper strip is taken as PZT-4 material constants of which are $c_{44}=2.56\times10^{10}\,\mathrm{N/m^2}$, $e_{15}=12.7\mathrm{C/m^2}$, $\varepsilon_{11}=64.63\times10^{-10}\,\mathrm{C/Vm}$ and $\rho=7.5\times10^{3}\,\mathrm{kg/m^3}$. As the effects of electric load and geometry of crack configuration on dynamic response are investigated, the lower strip is taken as $BaTiO_3$ material constants of which are $c_{44}=4.4\times10^{10}\,\mathrm{N/m^2}$, $e_{15}=11.4\mathrm{C/m^2}$, $\varepsilon_{11}=128.3\times10^{-10}\,\mathrm{C/Vm}$ and $\rho=5.7\times10^{3}\,\mathrm{kg/m^3}$. And as the effects of material property parameters are investigated, except for the variation of the material constant pointed out in the corresponding figures, all the other material constants of the lower strip are respectively set to be equal to that of the upper strip, i.e. PZT-4. Without any loss in generality, in all our numerical procedure, we take $\tau_0=4.2\times10^{6}\,\mathrm{N/m^2}$, and determine D_0 by λ through Eq. (87).

The normalized DSIF and DERR in the case of electric impermeable interface cracks subjected to the shear impact are presented in Figs. 2(a) and (b), respectively. For this loading case, the DEDIF at the crack tip, i.e. $x = a$ or $x = b$ is equal to zero. Therefore, the DSIF and DERR as indicators for possible crack initiation and growth play the same role in the case where only the shear impact is imposed. Figs. 2(a) and (b) indicate that both the DSIF and the DERR at $x = a$ are higher than that at $x = b$. And it is found that for given crack configuration and material pair, this is a common phenomenon for the coplanar interface cracks.

To illustrate the influence of the dynamic electric load on the interface crack extension force, the normalized DSIF and DERR at $x = a$ verse normalized time as a function of λ for PZT-4/$BaTiO_3$ are plotted in Figs. 3(a) and (b), respectively. As shown in Fig.3 (a), at the beginning of the impact process, the higher value of λ leads to lower value of DSIF, then the higher value of λ leads to higher value of DSIF. After three times of oscillating, the value of DSIF finally varies little as a function of λ for the given geometry parameters and material constants. Fig. 3(b) shows λ has different effects on DERR. In particular, at $t = 0$, the DERR is negative in the presence of electric field, and the DERR for a fixed value λ equals to that for $-\lambda$. Because the electric fields have contributed to the DERR as the impermeable case is considered, the DERR is more appropriate to be taken as fracture parameter than the DSIF in the view of fracture mechanics. All these results also imply that, on one hand, the electrical load promotes or retards crack growth depending on both the magnitude and the direction of electrical load. On the other hand, the negative electric impact is

more liable to promote the crack initiation and growth. In addition, numerical results show that for given geometry of crack configuration and combination of material parameters, the DEDIFs at the crack tips are proportional to λ, and do not vary with time.

Figs. 4-6 show the effects of the sizes of piezoelectric strips on the DERR of both electric impermeable and electric permeable interface cracks. From these figures, it can be clearly seen that for the given material pair, PZT-4/$BaTiO_3$, there are no distinct differences for the two kinds of electric boundaries in the absence of electric impact. However, the peak value corresponding to electric permeable interface cracks is higher than that corresponding to electric impermeable case. For two equal thickness' piezoelectric strips, as shown in Figs. 4(a) and (b), with the value of H_1/c increasing, both the number of resonance peak of DERR and the corresponding main peak value decrease, thus, the oscillation will become weaker. It should be noted that as $H_1/c \to \infty$, the results obtained are in fact that of two coplanar cracks between two dissimilar half-infinite piezoelectric materials. For a fixed value of H_1/c, Figs. 5(a) and (b) indicate that the oscillation also becomes weaker with the ratio of strip's thickness increasing. And as the ratio tends to infinity, the corresponding results reflect the dynamic properties of interface cracks between a half-infinite piezoelectric material and its bonded strip. From Fig. 6, we can easily know that the peak value of DERR decreases with the value of a/c increasing. That is, the larger the distance between the two cracks, the weaker the oscillation is. Moreover, the relative crack

separation has little effect on normalized time of reaching the corresponding static value.

As shown in Figs. 7-10, material constants have significant influences on DERR for both electric impermeable and electric permeable cases. In general, the peak value of DERR for electric permeable interface cracks is much higher than that for electric impermeable cracks, and the effects of piezoelectric constant and dielectric constant on DERR for electric permeable interface cracks have different properties to that for electric impermeable cracks.

5. Conclusions

In this article, the transient response of two coplanar interface cracks between two dissimilar piezoelectric strips under dynamic electromechanical loads is investigated. Two kinds of electric boundary conditions are adopted. Laplace and Fourier transforms and dislocation density functions are used to reduce the mixed boundary value problem to a system of Cauchy singular equations. The DSIF and DERR are calculated and discussed. From the numerical results presented in this paper, the following conclusions may be drawn.

For both electric impermeable and electric permeable boundary conditions, the DERR and DSIF at the inner crack tip are always larger than the DERR and DSIF at the outer tip. In other words, under electromechanical impact, the coplanar cracks tend to propagate at first from inner crack tips. For both electric impermeable cracks when only shear impact is applied and the electric permeable interface cracks, the DERR and DSIF are equivalent in view of fracture mechanics. However, for electric

impermeable crack under mechanical and electrical impacts, the DERR as the fracture parameter can reflect more accurate properties than the DSIF, and properly adjusting electric load can retard the crack initiation and growth. For both electric impermeable and permeable cases, geometry criterion of piezoelectric strips, relative crack separation and material constants, all have great and different influences on the DERR. And the effects of material constants especially piezoelectric and dielectric constants are more sensitive than that of crack configuration to the two kinds of electric boundary conditions. In addition, the transient responses of interface cracks both between two half-infinite piezoelectric materials and between a half-infinite piezoelectric material and its bonded strip are the particular cases of the problem studied in this paper.

Acknowledgement

This research was supported by the grant from the Research Grants Council of the Hong Kong Special Administrative Region, China under project No. HKU 7014/00E and the National Natural Science Fund of China under project No. 19772029.

Appendix A

$$a_{11} = -a_{12} = -\tilde{c}_{44(1)}\alpha_{(1)},\ a_{13} = -a_{14} = -e_{15(1)}s$$

$$a_{15} = -a_{16} = \tilde{c}_{44(2)}\alpha_{(2)},\ a_{17} = -a_{18} = e_{15(2)}s$$

$$a_{21} = a_{22} = a_{25} = a_{26} = 0,\ a_{23} = -a_{24} = \varepsilon_{11(1)}s,\ a_{27} = -a_{28} = -\varepsilon_{11(2)}s$$

$$a_{31} = -\tilde{c}_{44(1)}\alpha_{(1)}\exp\left(-\alpha_{(1)}h_1\right),\ a_{32} = \tilde{c}_{44(1)}\alpha_{(1)}\exp\left(\alpha_{(1)}h_1\right)$$

$$a_{33} = -e_{15(1)}s\exp\left(-sh_1\right),\ a_{34} = e_{15(1)}s\exp\left(sh_1\right),\ a_{35} = a_{36} = a_{37} = a_{38} = 0$$

$$a_{41} = -\tilde{c}_{44(2)}\alpha_{(2)}\exp(\alpha_{(2)}h_2),\ a_{42} = \tilde{c}_{44(2)}\alpha_{(2)}\exp(-\alpha_{(2)}h_2)$$

$$a_{43} = -e_{15(2)}s\exp(sh_2),\ a_{44} = e_{15(2)}s\exp(-sh_2),\ a_{45} = a_{46} = a_{47} = a_{48} = 0$$

$$a_{51} = a_{52} = a_{55} = a_{56} = a_{57} = a_{58} = 0$$

$$a_{53} = \varepsilon_{11(1)}s\exp(-sh_1),\ a_{54} = -\varepsilon_{11(1)}s\exp(sh_1)$$

$$a_{61} = a_{62} = a_{63} = a_{64} = a_{65} = a_{66} = 0$$

$$a_{67} = \varepsilon_{11(2)}s\exp(sh_2),\ a_{68} = -\varepsilon_{11(2)}s\exp(-sh_2)$$

$$a_{71} = a_{72} = -a_{75} = -a_{76} = 1,\ a_{73} = a_{74} = a_{77} = a_{78} = 0$$

$$a_{81} = a_{82} = e_{15(1)}/\varepsilon_{11(1)},\ a_{85} = a_{86} = -e_{15(2)}/\varepsilon_{11(2)},\ a_{83} = a_{84} = -a_{87} = -a_{88} = 1$$

Appendix B

$$\gamma_{11} = \frac{\tilde{c}_{44(1)}e_{15(2)}{}^2\varepsilon_{11(1)}{}^2 + \tilde{c}_{44(2)}e_{15(1)}{}^2\varepsilon_{11(2)}{}^2 - \tilde{c}_{44(1)}\tilde{c}_{44(2)}\varepsilon_{11(1)}\varepsilon_{11(2)}(\varepsilon_{11(1)} + \varepsilon_{11(2)})}{\gamma}$$

$$\gamma_{12} = -\frac{\tilde{c}_{44(1)}e_{15(2)}\varepsilon_{11(1)}{}^2\varepsilon_{11(2)} + \tilde{c}_{44(2)}e_{15(1)}\varepsilon_{11(1)}\varepsilon_{11(2)}{}^2}{\gamma} = \gamma_{21}$$

$$\gamma_{22} = \frac{(\tilde{c}_{44(1)} + \tilde{c}_{44(2)})\varepsilon_{11(1)}{}^2\varepsilon_{11(2)}{}^2}{\gamma}$$

$$\gamma = e_{15(2)}{}^2\varepsilon_{11(1)}{}^2 + e_{15(1)}{}^2\varepsilon_{11(2)}{}^2 - (\tilde{c}_{44(1)} + \tilde{c}_{44(2)})\varepsilon_{11(1)}\varepsilon_{11(2)}(\varepsilon_{11(1)} + \varepsilon_{11(2)}) - 2e_{15(1)}e_{15(2)}\varepsilon_{11(1)}\varepsilon_{11(2)}$$

$$Q_{11}(v,x,p) = \frac{\gamma_{11}}{v+x} + \int_0^{+\infty}\left(\frac{-P_{11}(s,p)}{s\Delta(s,p)} - \gamma_{11}\right)[\sin s(v-x) + \sin s(v+x)]ds$$

$$Q_{12}(v,x,p) = \frac{\gamma_{12}}{v+x} + \int_0^{+\infty}\left(\frac{-P_{12}(s,p)}{s\Delta(s,p)} - \gamma_{12}\right)[\sin s(v-x) + \sin s(v+x)]ds$$

$$Q_{21}(v,x,p) = \frac{\gamma_{21}}{v+x} + \int_0^{+\infty}\left(\frac{-P_{21}(s,p)}{s\Delta(s,p)} - \gamma_{21}\right)[\sin s(v-x) + \sin s(v+x)]ds$$

$$Q_{22}(v,x,p) = \frac{\gamma_{22}}{v+x} + \int_0^{+\infty}\left(\frac{-P_{22}(s,p)}{s\Delta(s,p)} - \gamma_{22}\right)[\sin s(v-x) + \sin s(v+x)]ds$$

$$F(\eta, p) = f\left(\frac{b-a}{2}\eta + \frac{b+a}{2}, p\right)$$

$$G(\eta, p) = g\left(\frac{b-a}{2}\eta + \frac{b+a}{2}, p\right)$$

$$\tilde{Q}_{ij}(\eta, \varsigma, p) = \frac{b-a}{2} Q_{ij}\left(\frac{b-a}{2}\eta + \frac{b+a}{2}, \frac{b-a}{2}\varsigma + \frac{b+a}{2}, p\right) \quad (i, j = 1,2)$$

References

[1] Parton, V.: Fracture mechanics of piezoelectric materials. Acta Astronaut. **3,** 671-683 (1976).

[2] Deeg, W.: The analysis of dislocation, crack, and inclusion problems in piezoelectric solids. Ph.D. Thesis, Stanford University, 1980.

[3] Khutoryansky, N., Sosa, H.: Dynamic representation formula and fundamental solutions for piezoelectricity. Int. J. Solids Struct. **32,** 3307-3325 (1995).

[4] Ding, H., Chen, B., Liang, J.: General solutions for coupled equations for piezoelectric media. Int. J. Solids Struct. **33,** 2283-2298 (1996).

[5] Dascalu, C., Maugin, G.: On the dynamic fracture of piezoelectric materials. Q. J. Mech. Appl. Math. **48,** 237-255 (1995).

[6] Li, S., Mataga, P.: Dynamic crack propagation in piezoelectric materials. Part Ⅰ: Electrode solution. J. Mech. Phys. Solids **44,** 1799-1830 (1996).

[7] Li, S., Mataga, P.: Dynamic crack propagation in piezoelectric materials. Part Ⅱ: Vacuum solution. J. Mech. Phys. Solids **44,** 1831-1866 (1996).

[8] Chen, Z.: Crack-tip field of an infinite piezoelectric strip under anti-plane impact. Mech. Res. Commun. **25,** 313-319 (1998).

[9] Chen, Z., Karihaloo, B. H.: Dynamic response of a cracked piezoelectric ceramic under arbitrary electro-mechanical impact. Int. J. Solids Struct. **36,** 5125-5133 (1999).

[10] Chen, Z., Yu, S.: A semi-infinite crack under anti-plane mechanical impact in piezoelectric materials. Int.J. Fract. **88,** L53-L56 (1998).

[11] Chen, Z., Yu, S.: Transient response of a piezoelectric ceramic with two coplanar cracks under electromechanical impact. Acta Mech. Sinica (English Series) **15,** 325-333 (1999).

[12] Wang, X., Yu, S.: Transient response of a crack in piezoelectric strip subjected to the mechanical and electrical impacts: mode III problem. Int. J. Solids Struct. **37,** 5795-5808 (2000).

[13] Wang, B. L., Han, J. C., Du, S. Y.: Electroelastic fracture dynamics for multilayered piezoelectric materials under dynamic anti-plane shearing. Int. J. Solids Struct. **37,** 5219-5231 (2000).

[14] Kwon, S. M., Lee, K. Y.: Transient response of a rectangular medium with a center crack. Eur. J. Mech. A/Solids **20,** 457-468 (2000).

[15] Li, X.: Transient response of a piezoelectric material with a semi-infinite mode Ⅲ crack under impact loads. Int. J. Fract. **111,** 119-130 (2001).

[16] Li, X., Fan, T.: Transient analysis of a piezoelectric strip with a permeable crack under anti-plane impact loads. Int. J. Eng. Sci. **40,** 131-143 (2001).

[17] Shindo, Y., Katsura, H., Yan, W.: Dynamic stress intensity factor of a cracked electric medium in a uniform electric field. Acta Mech. **117,** 1-10 (1996).

[18] Narita, F., Shindo, Y.: Scattering of Love waves by a surface-breaking crack in piezoelectric layered medium. JSME Int. J. **41,** 40-48 (1998).

[19] Wang, X., Yu, S.: Scattering of SH waves by an arc-shaped crack between a cylindrical piezoelectric inclusion and matrix-II: far fields. Int. J. Fract. **100**, L35-L40 (1999).

[20] Pak, Y.: Crack extension force in a piezoelectric material. ASME J. Appl. Mech. **57**, 647-653 (1990).

[21] Erdogan, F., Ozbek, T.: Stresses in fiber-reinforced composites with imperfect bonding. ASME J. Appl. Mech. **36**, 865-869 (1969).

[22] Muskhelisvili, N. I.: Singular Integral Equations. Groningen: Noordhoff 1953.

[23] Erdogan, F., Gupta, G. D.: On the numerical solution of singular integral equations. Q. Appl. Math. **29**, 525-539 (1972)

[24] Miller, M., Guy, W.: Numerical inversion of the Laplace transform by use of Jacobi polynomials. SIAM J. Num. Anal. **3**, 624-635 (1966).

[25] McMeeking, R.: On mechanical stress at cracks in dielectrics with application to dielectric breakdown. J. Appl. Phys. **62**, 3116-3122 (1989).

Authors' addresses:

R. K. L. Su, Department of Civil Engineering, The University of Hong Kong, Pokfulam Road, Hong Kong, People's Republic of China

W. J. Feng and **J. X. Liu**, Department of Mechanics and Engineering Science, Shijiazhuang Railway Institute, Shijiazhuang 050043, People's Republic of China

Z. Z. Zou, Department of Engineering Mechanics, Harbin Institute of Technology, Harbin, 150001, People's Republic of China

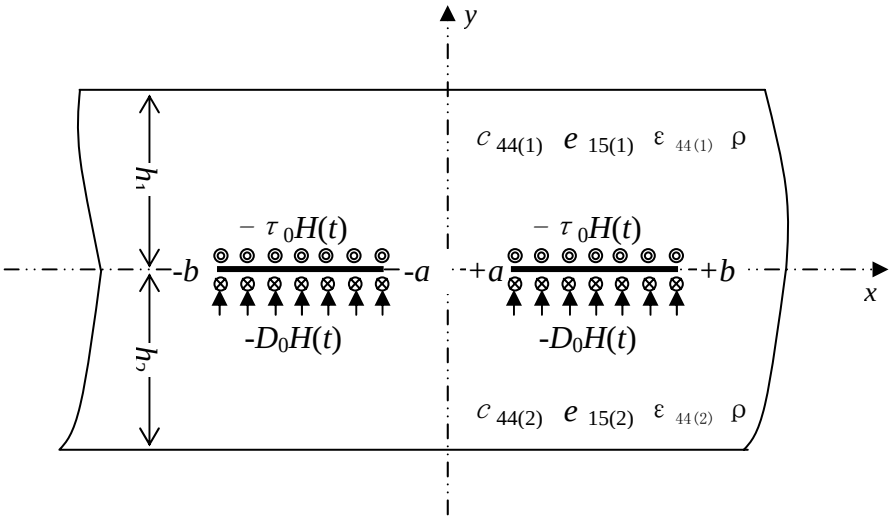

Fig. 1. Two dissimilar piezoelectric strips with two coplanar interface cracks under anti-plane mechanical impact and electrical impact

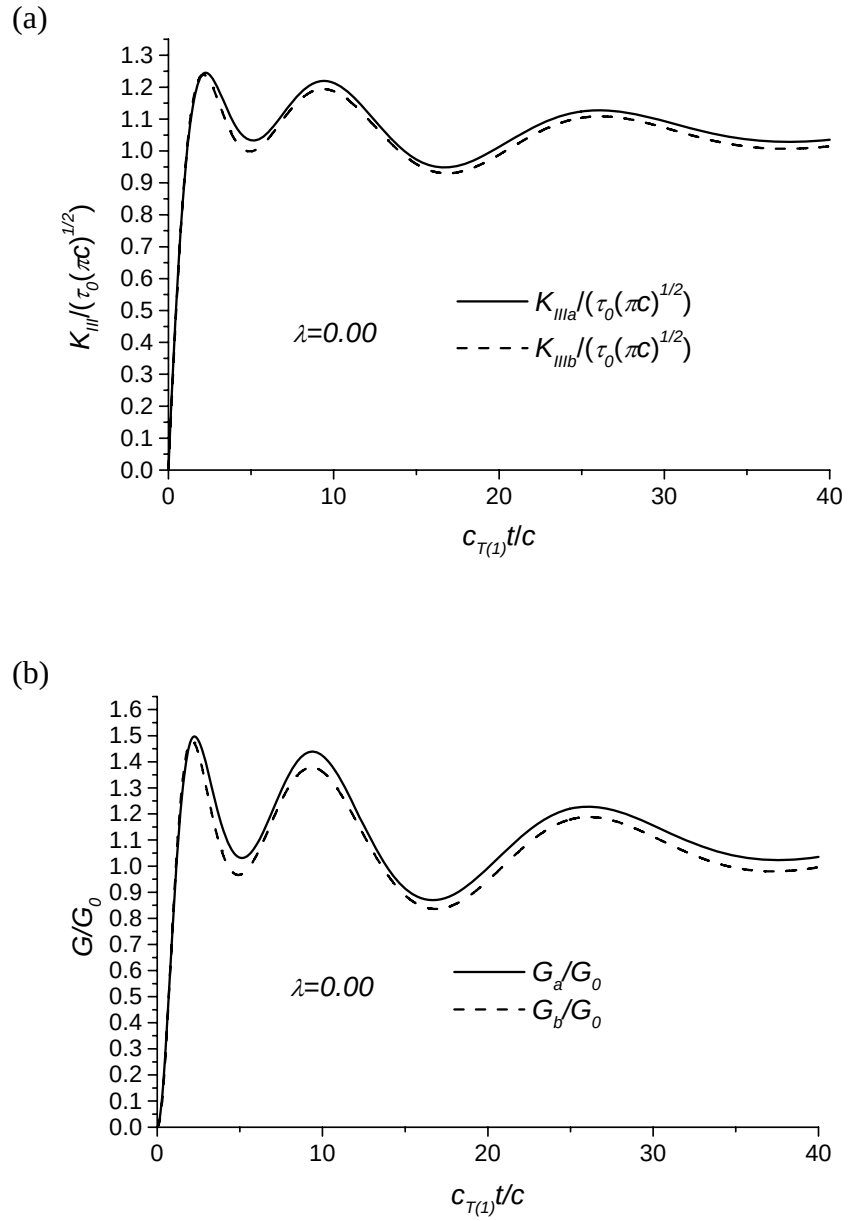

Fig. 2. Normalized dynamic stress intensity factors and energy release rates at $x=a$ and $x=b$ with normalized time for electric impermeable interface cracks under shear impact, PZT-4/$BaTiO_3$, $a/c=1$, $h_2/h_1=1$, $h_1/c=5$

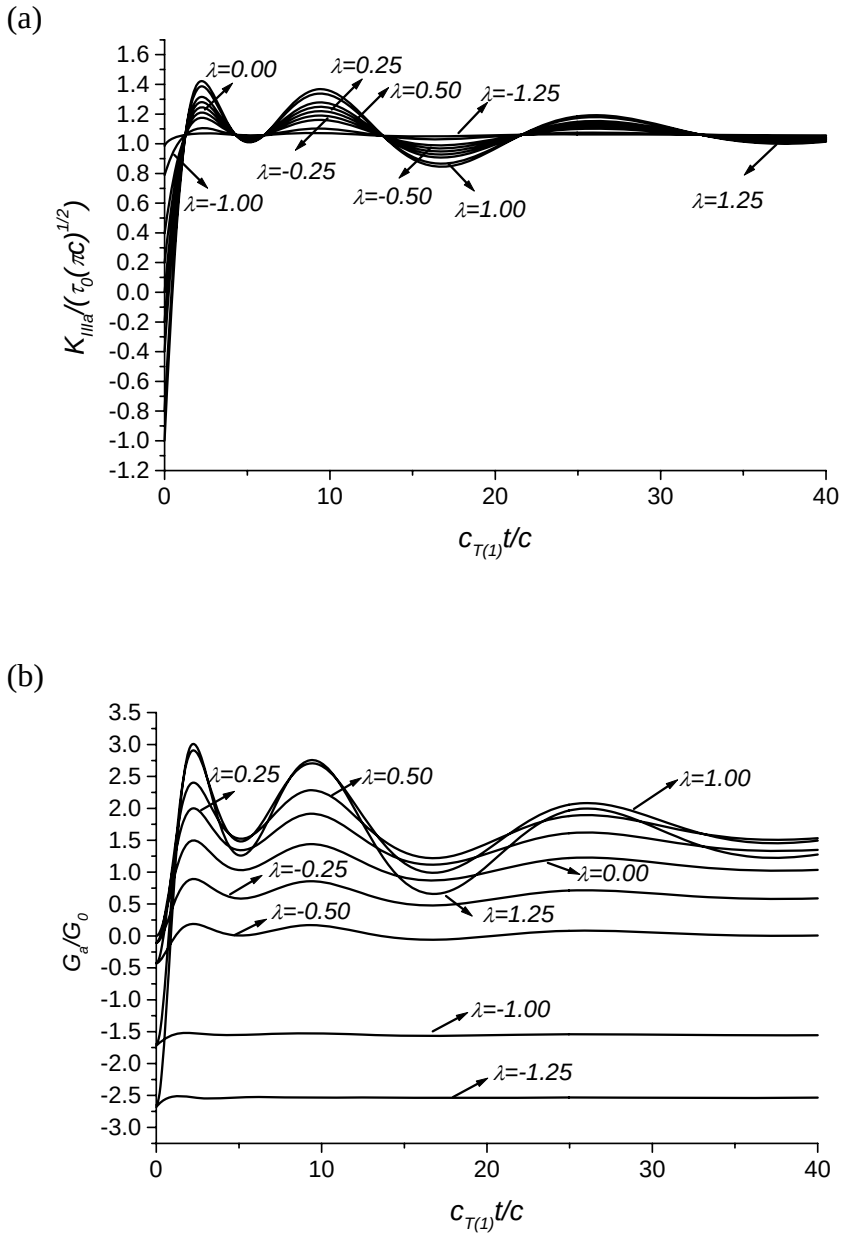

Fig. 3. Normalized dynamic stress intensity factors and energy release rates for various load combination parameters with normalized time for electric impermeable interface cracks, PZT-4/$BaTiO_3$, $a/c=1$, $h_2/h_1=1$, $h_1/c=5$

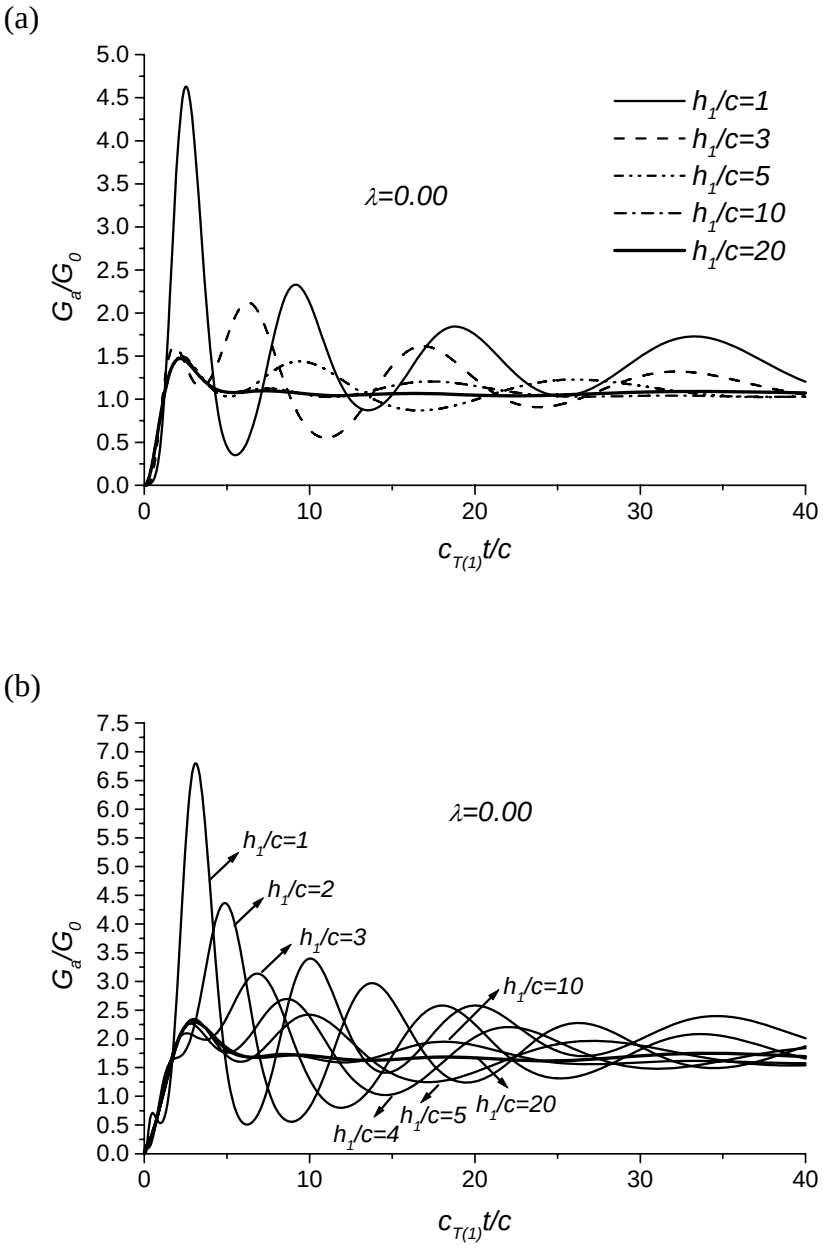

Fig. 4. Normalized dynamic energy release rates for various width's piezoelectric strips as $h_2/h_1=1$ with normalized time under shear impact, PZT-4/$BaTiO_3$, $a/c=1$: (a) electric impermeable cracks; (b) electric permeable cracks

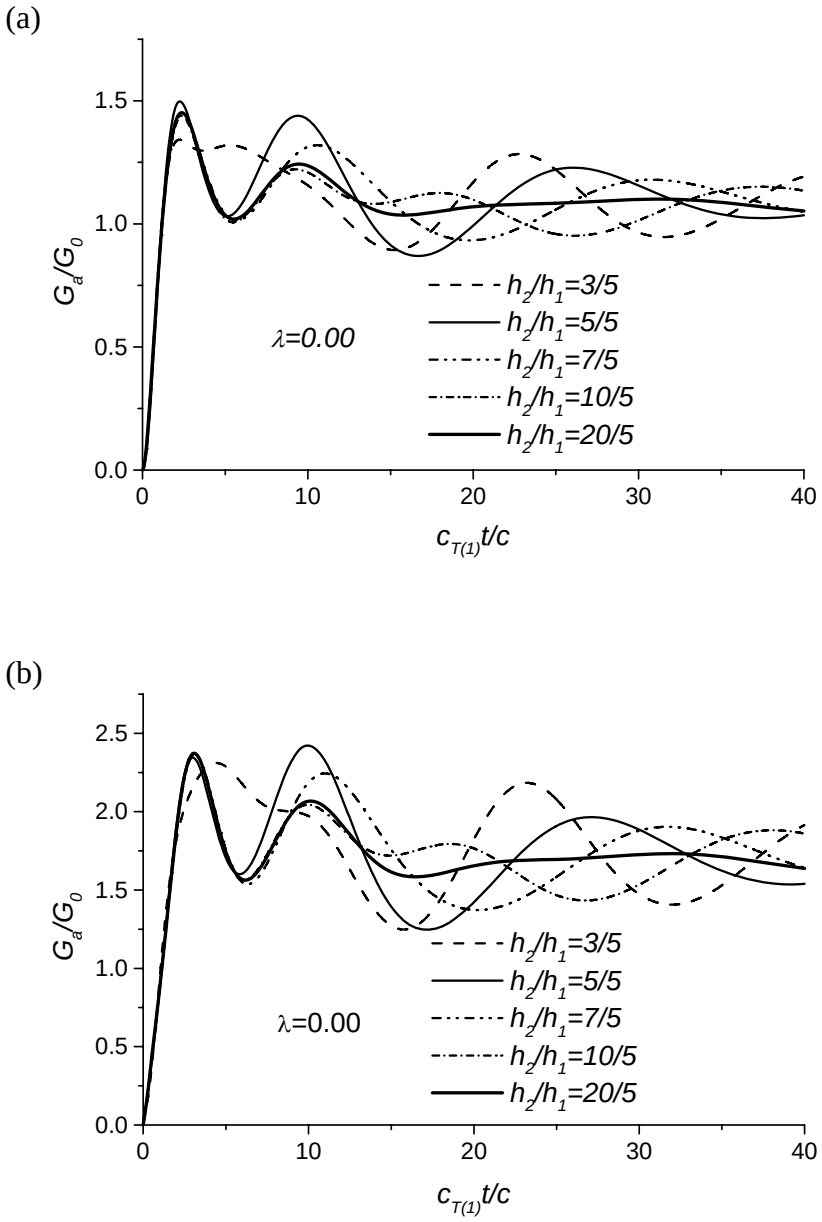

Fig. 5. Normalized dynamic energy release rates for various ratios of h_2/h_1 as $h_1/c=5$ with normalized time under shear impact, PZT-4/$BaTiO_3$, $a/c=1$: (a) electric impermeable cracks; (b) electric permeable cracks

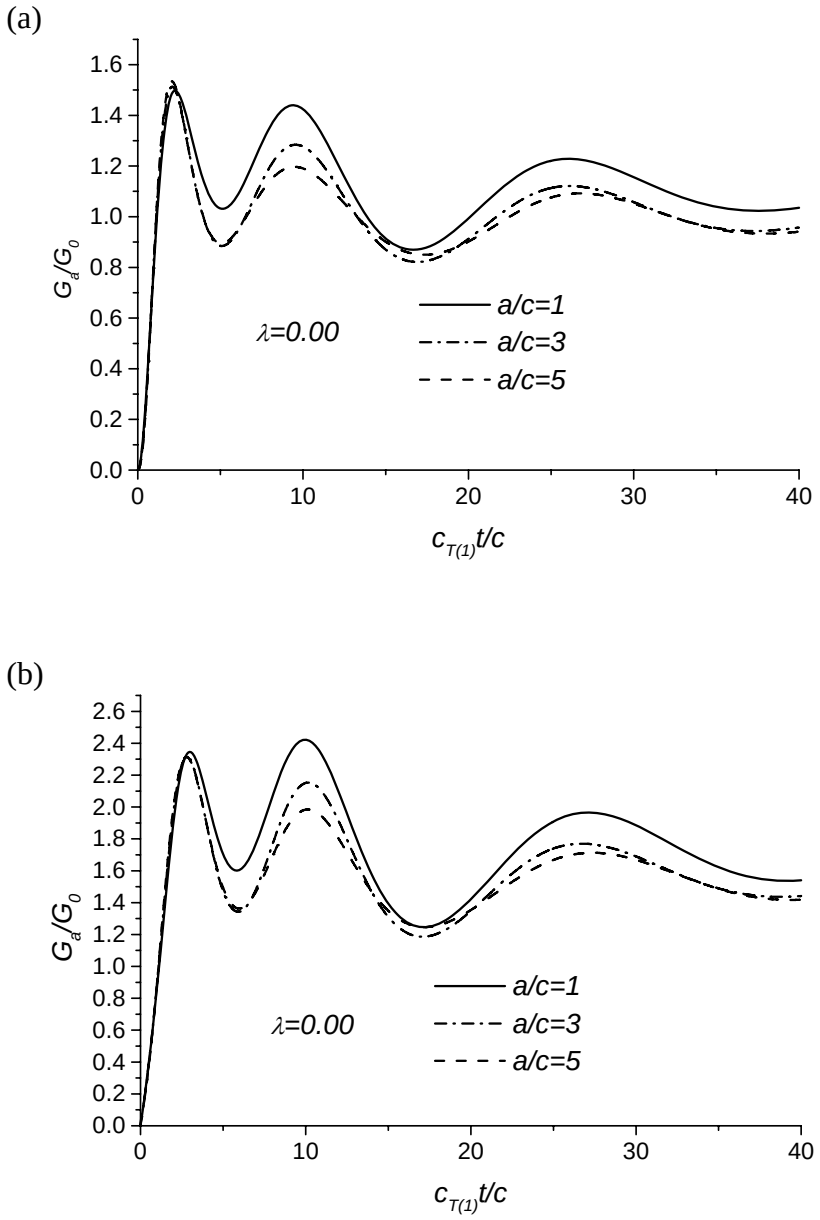

Fig. 6. Normalized dynamic energy release rates for different relative crack positions with normalized time under shear impact, PZT-4/$BaTiO_3$, $h_2/h_1=1$, $h_1/c=5$: (a) electric impermeable cracks; (b) electric permeable cracks

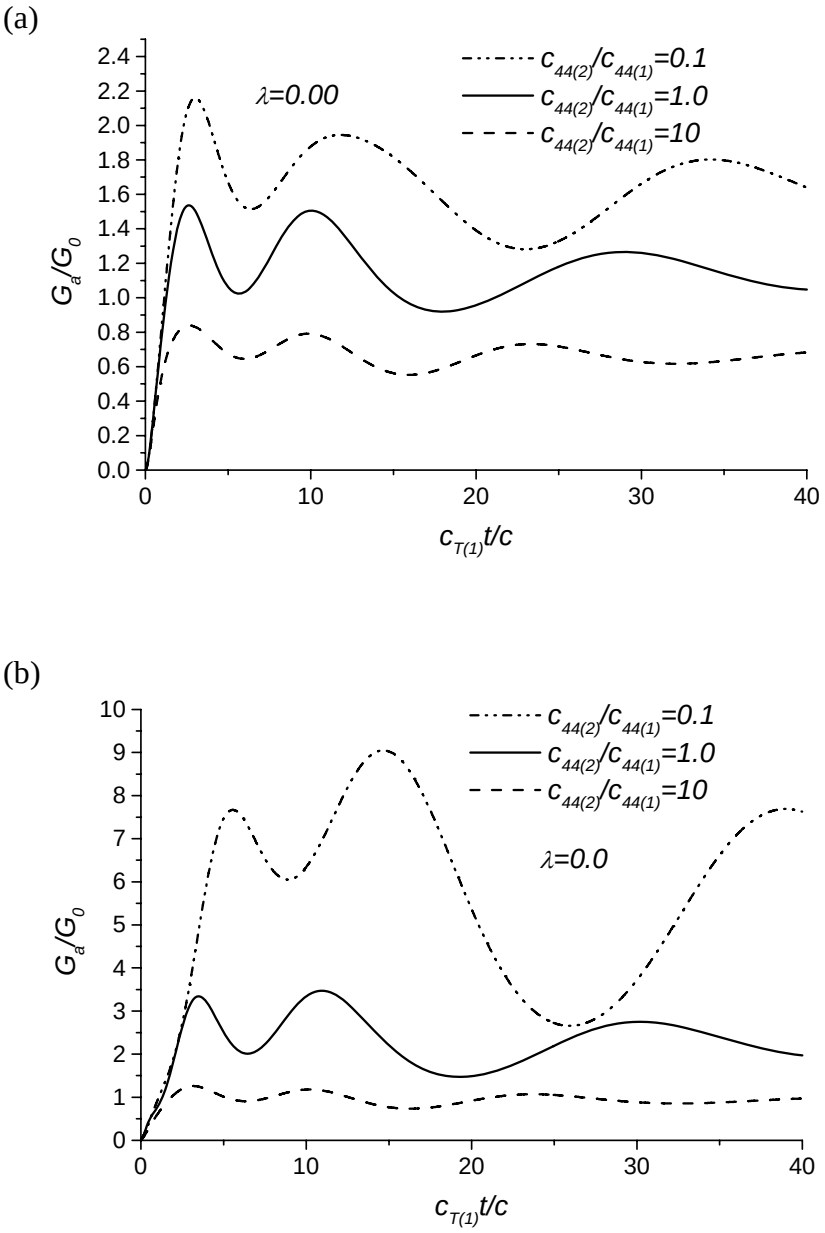

Fig. 7. Normalized dynamic energy release rates for various ratios of elastic constants with normalized time under shear impact, $a/c=1$, $h_2/h_1=1$, $h_1/c=5$: (a) electric impermeable cracks; (b) electric permeable cracks

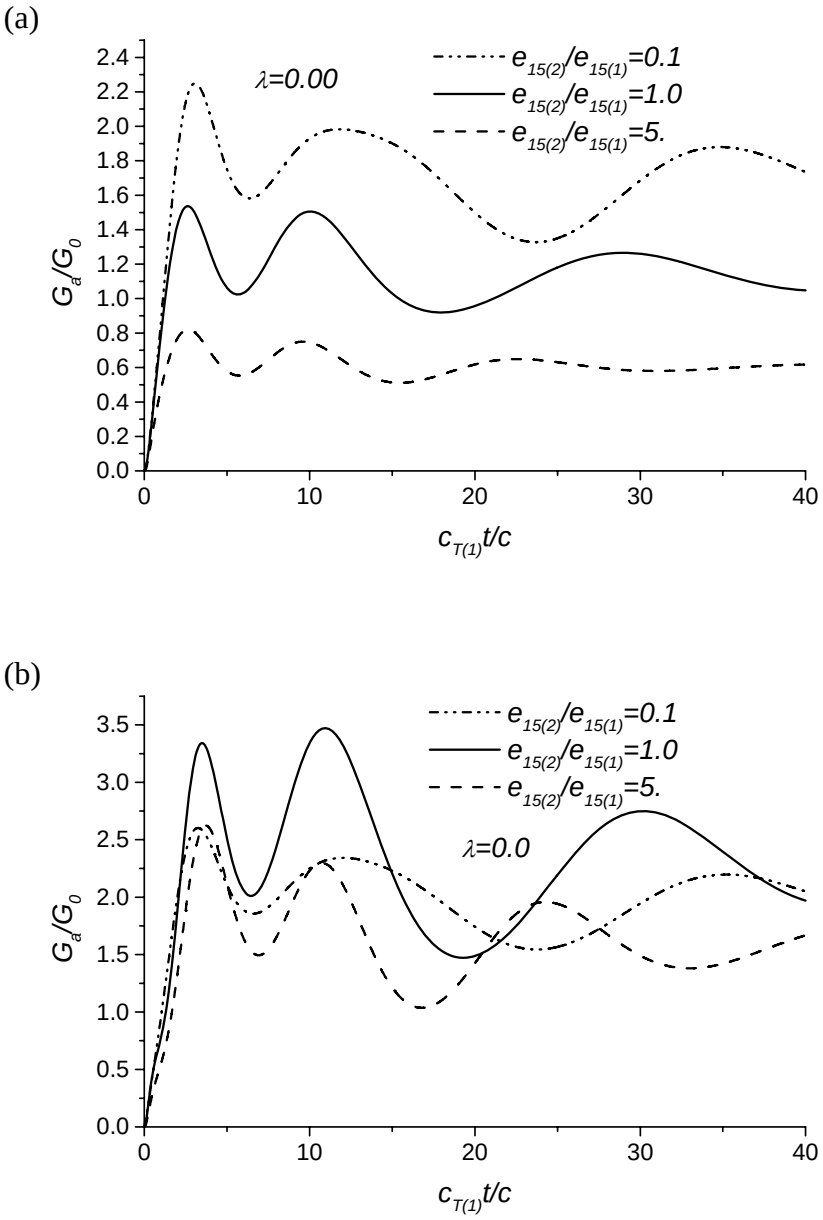

Fig. 8. Normalized dynamic energy release rates for various ratios of piezoelectric constants with normalized time under shear impact, $a/c=1$, $h_2/h_1=1$, $h_1/c=5$: (a) electric impermeable cracks; (b) electric permeable cracks

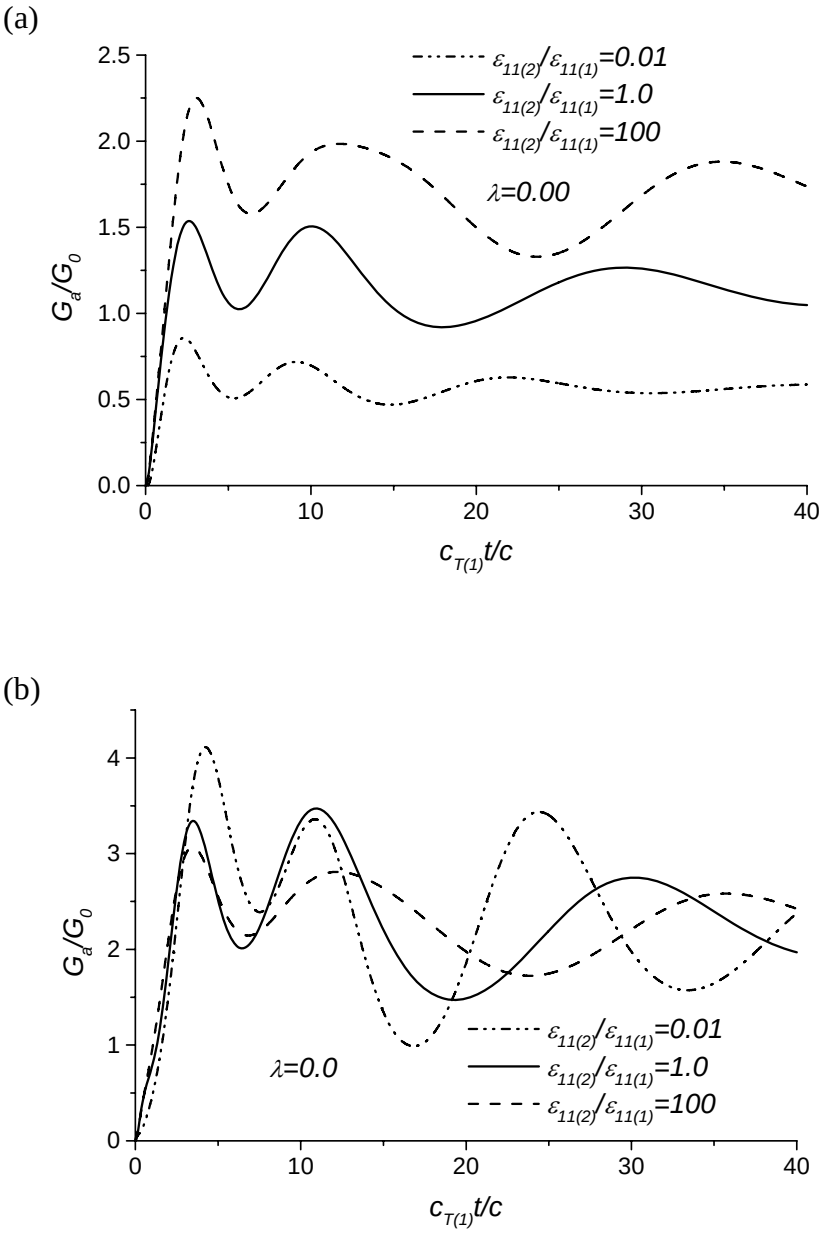

Fig. 9. Normalized dynamic energy release rates for various ratios of dielectric constants with normalized time under shear impact, $a/c=1$, $h_2/h_1=1$, $h_1/c=5$: (a) electric impermeable cracks; (b) electric permeable cracks

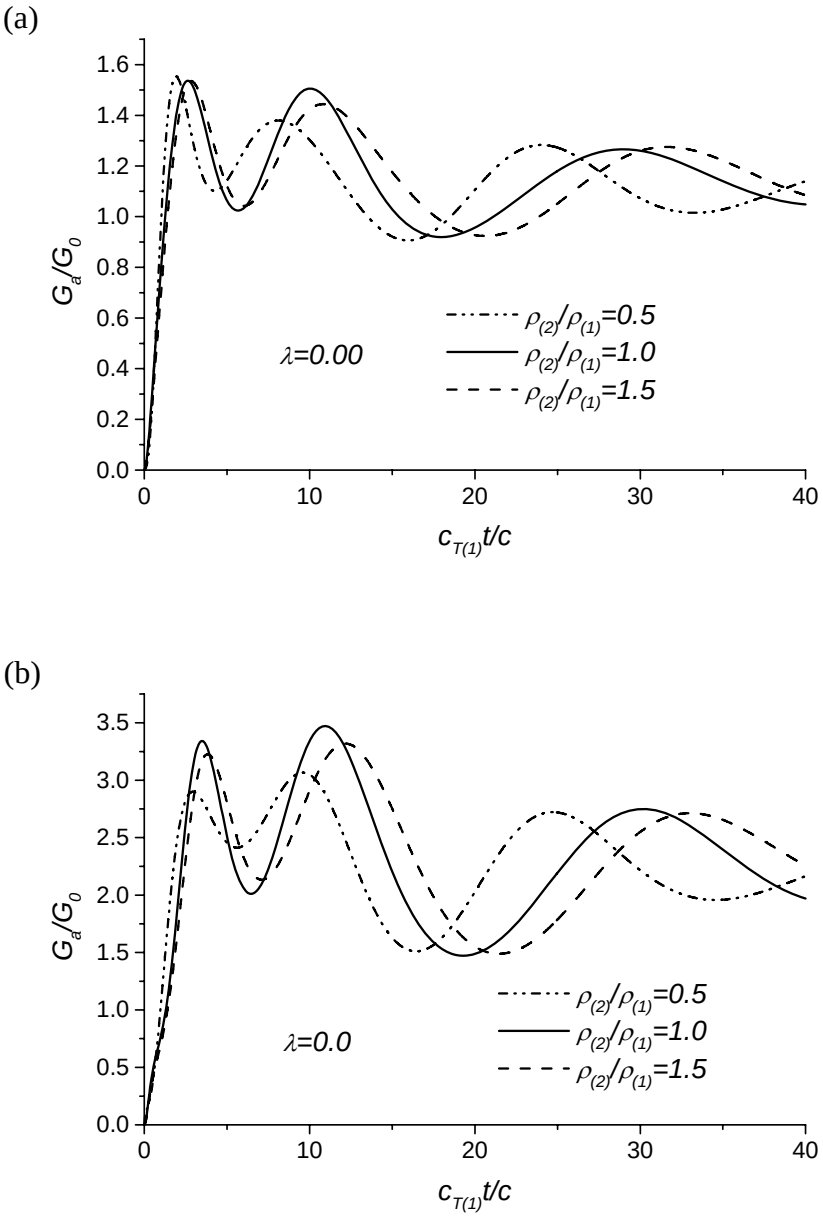

Fig. 10. Normalized dynamic energy release rates for various ratios of material densities with normalized time under shear impact, $a/c=1$, $h_2/h_1=1$, $h_1/c=5$: (a) electric impermeable cracks; (b) electric permeable cracks